sensors

MDPI

Article

As-Doped h-BN Monolayer: A High Sensitivity and Short Recovery Time SF_6 Decomposition Gas Sensor

Yunfeng Long †, Sheng-Yuan Xia †, Liang-Yan Guo, Yaxiong Tan * and Zhengyong Huang

State Key Laboratory of Power Transmission Equipment and System Security and New Technology, School of Electrical Engineering, Chongqing University, Chongqing 400044, China; 15200879239@163.com (Y.L.); xiashengyuan@cqu.edu.cn (S.-Y.X.); guoliangyanself@163.com (L.-Y.G.); huangzhengyong@cqu.edu.cn (Z.H.)

* Correspondence: yxtan@cqu.edu.cn

† These authors contributed equally to this work.

Abstract: SF_6 is a common insulating medium of gas-insulated switchgear (GIS). However, it is inevitable that SF_6 will be decomposed due to partial discharge (PD) in GIS, which will cause hidden dangers to the safe and stable operation of equipment. Based on the DFT method, the two-dimensional nano-composite As-doped h-BN (As-BN) monolayer was proposed. By modeling and calculating, the ability of an As-BN monolayer as a specific sensor for SO_2F_2 (compared with an H_2O adsorption system and CO_2 adsorption system) was evaluated by parameters such as the binding energy (E_b), adsorption energy (E_{ads}), transfer charge (ΔQ), geometric structure parameters, the total density of states (TDOS), band structure, charge difference density (CDD), electron localization function (ELF), sensitivity (S), and recovery time (τ). The results showed that an As-BN monolayer showed strong adsorption specificity, high sensitivity, and short recovery time for SO_2F_2 gas molecules. Therefore, the As-BN monolayer sensor has great application potential in the detection of SF_6 decomposition gases.

Keywords: SF_6 decomposition gas; gas sensor; As-BN monolayer; DFT

Citation: Long, Y.; Xia, S.-Y.; Guo, L.-Y.; Tan, Y.; Huang, Z. As-Doped h-BN Monolayer: A High Sensitivity and Short Recovery Time SF_6 Decomposition Gas Sensor. *Sensors* **2022**, *22*, 4797. https://doi.org/10.3390/s22134797

Academic Editor: Sang Sub Kim

Received: 7 June 2022
Accepted: 24 June 2022
Published: 24 June 2022

1. Introduction

SF_6 gas is widely used in gas-insulated switchgear (GIS) due to its high dielectric strength, excellent arc extinguishing ability, and good insulation characteristics [1–3]. However, some insulation defects, such as partial discharge (PD), are inevitable during the long-term operation of GIS. The PD is the fault characteristic phenomenon before the complete breakdown or flashover of GIS insulation, and it is also the early manifestation of GIS internal insulation defects, causing great hidden dangers to the safe and stable operation of GIS. Under the continuous action of PD, a variety of low-fluorine sulfides formed by SF_6 decomposition will react with H_2O molecules, which will lead to the decomposition of the SF_6 gas which is difficult to reduce, and generate SO_2F_2 and other SF_6 decomposition gases [4–7]. This will significantly reduce the insulation performance of SF_6 gas and accelerate the deterioration of GIS insulation, which may lead to sudden faults in the operation of GIS. Therefore, the monitoring of SF_6 decomposition gas is of great significance to the defect identification and early warning of GIS.

At present, the traditional methods for detecting SF_6 decomposition gases produced by PD in GIS include chromatography and spectroscopy [8–11]. The basic principle of chromatography is to push the mixed gas samples taken from GIS into the chromatographic column, separate SF_6 decomposition gases by using different gas adsorption or dissolution capacities of each component and identify and calibrate them with special detectors. However, this method is relatively complex, high instrument price has high requirements for operators, and cannot realize online monitoring. Spectroscopy is a quantitative detection of SF_6 decomposition gases by using the relationship between the absorption degree of different measured gases and the volume fraction of the gas. However, the spectral method has low sensitivity and low detection accuracy in the detection of trace gases, and there is a

cross-interference between the absorption peak of SF_6 and its decomposed components. More importantly, with both spectroscopy and chromatography, it is difficult to achieve online monitoring of SF_6 decomposition gases. Therefore, it is very important to develop real-time, accurate, convenient, and intelligent SF_6 decomposition gas monitoring technology.

With the rapid development of nanotechnology, the gas sensor method has made rapid progress. The basic principle of gas sensors based on nanomaterials is that when detecting gas, nanomaterials, such as graphene, boron nitride, and carbon nanotubes, interact with gas, resulting in varying degrees of electrical signal response to calculate the type, concentration, and gas production rate of gas [12–16]. It has the advantages of low preparation cost, simple process, fast detection speed, high sensitivity, and real-time monitoring. At present, most studies on the monitoring of SF_6 decomposition gases by gas sensor method are mainly common gases, such as SO_2 and H_2S, but the exploration of important gas components such as SO_2F_2 is still relatively small [17–20]. Therefore, it is necessary to further develop gas sensors that can cover SO_2F_2 and other major SF_6 decomposition gases. With the development of computer science, the DFT method based on quantum mechanics has been widely used in the field of gas sensing [21–32]. According to previous research, the material properties calculated by the DFT method have high consistency with the experimental results, which confirms the feasibility of this method in the field of gas sensing.

In this study, we proposed a novel As-doped h-BN (As-BN) monolayer gas sensor for SF_6 decomposition gas monitoring. Based on the DFT method, the gas sensing response mechanism of the interaction between As-BN monolayer and SO_2F_2 gas molecules was discussed at the micro-level. Considering the fact that SF_6 gas molecules are more likely to produce SO_2F_2 gas in the presence of gases such as H_2O molecules in the air, the gas sensing response parameters with As-BN monolayer and H_2O and CO_2 gas molecules are also explored. This study provides a theoretical basis for the preparation of an As-BN monolayer gas sensor for SF_6 decomposition gas detection and provides a convenient way for the development of other sensors.

2. Computational Details

Based on the DFT method, the construction and calculation of the model in this study are all in DMol3 and CASTEP codes of the Materials Studio software [33–36]. In order to avoid the interference of adjacent units, a 15 Å vacuum layer was constructed. The Perdew-Burke-Ernzehof (PBE) of the generalized gradient approximation (GGA) is selected to better deal with the inter-electron exchange-correlation functional. DFT semi-core pseudo-potential (DSPP) is used to simplify the electronic interaction between atoms. At the same time, double numerical plus polarization (DNP) is also added as the basic function of the linear combination method of atomic orbitals. Considering the Van Der Waals forces in the process of impurity doping and gas adsorption and the interaction between long distances, the DFT-D2 method is used to analyze all models, which can effectively improve the calculation accuracy of the system. The k point, energy convergence accuracy, maximum force, and maximum displacement are set to $6 \times 6 \times 1$, 1×10^{-5} Ha, 2×10^{-3} Ha/Å, 5×10^{-3} Å.

In this study, the calculation formula of binding energy is as follows:

$$E_b = E_{\text{doped-BN}} + \mu_{B/N} - E_{BN} - \mu_{As} \quad (1)$$

where $E_{\text{doped-BN}}$ and E_{BN} represent the energy of the doped-BN monolayer and pristine h-BN monolayer, respectively; the μ represents the chemical potential of the counterpart elements. The calculated formation energies of As-BN monolayers doped with As atoms at positions 1 and 2 are 6.501 eV and 6.931 eV, respectively.

In this study, the adsorption energy formula is as follows:

$$E_{ads} = E_{\text{Gas/As-BN}} - E_{\text{Gas}} - E_{\text{As-BN}} \quad (2)$$

where $E_{Gas/As\text{-}BN}$, E_{Gas}, and $E_{As\text{-}BN}$ represent the energy of adsorption systems, gas molecule, and As-BN monolayer, respectively.

In this study, the calculation formula of transfer charge is as follows:

$$\Delta Q = Q_1 - Q_2 \quad (3)$$

where Q_1 and Q_2 represent the total charge of the gas molecule after and before adsorption, respectively.

In this study, the calculation formula of sensitivity is:

$$S = (1/\sigma_{As\text{-}BN/gas} - 1/\sigma_{As\text{-}BN})/(1/\sigma_{As\text{-}BN}) \quad (4)$$

where the $\sigma_{As\text{-}BN/gas}$ and $\sigma_{As\text{-}BN,}$ respectively, represent the conductivity of adsorption systems and As-BN monolayer.

In this study, the calculation formula of recovery time is:

$$\tau = {v_0}^{-1} \exp(-E_{ads}/kT) \quad (5)$$

where v_0, k, and T represent the attempt frequency, Boltzmann constant, and thermodynamic temperature, respectively.

3. Results and Discussion

Constructing appropriate h-BN monolayers is the basis for our subsequent research. As shown in Figure 1(a1,a2), we first constructed h-BN monolayers containing nine N atoms and nine B atoms in a $3 \times 3 \times 1$ supercell. The B-N bond length is 1.453 Å, and the B-N-B or N-B-N bond angle is about 120°. At the same time, other parameters are also similar to previous studies. Then, we doped the h-BN monolayer by substituting an As atom for an N atom (position 1) or a B atom (position 2). At the same time, we calculated the geometric structure parameters and binding energy (E_b) of the two after doping. Both are positive, indicating that the formation reactions of the two are endothermic reactions. The formation of the two needs to provide heat or other forms of energy in the outside world. The smaller formation energy of position 1 indicates that the doping method of one As atom instead of one N atom is more reliable and stable, while the doping method of position 2 is difficult to complete in the experiment. This may be related to the fact that an As atom has the same valence electron as an N atom. This makes an As atom replaces an N atom without an unpaired electron, and an As atom replacing a B atom will produce defects. From the perspective of geometric configuration, the B-N bond length of the b-BN monolayer (1.453 Å) is closer to the As-B bond length after doping in position 1 (l_1 = 1.848 Å) than that after doping in position 2 (l_2 = 2.000 Å). This indicates that the binding of an As atom at doping site 1 is closer than that at doping site 2, the change of bond length before doping is smaller, and a more stable structure can be formed. At the same time, the B-As-B bond angle (α_1 = 96.390°) formed by doping site 1 is closer to the B-N-B/N-B-N bond angle (120°) before doping than the N-As-N bond angle (α_2 = 94.138°) formed by doping site 2. The large change of bond angle will cause excessive distortion of the material, which will not be conducive to the stability of the material and the application of the function. Therefore, the adsorption of the three gas molecules (SO_2F_2, H_2O, and CO_2) explored in this study was based on an As atom to replace an N atom of the As-BN monolayer, as shown in Figure 1(b1,b2).

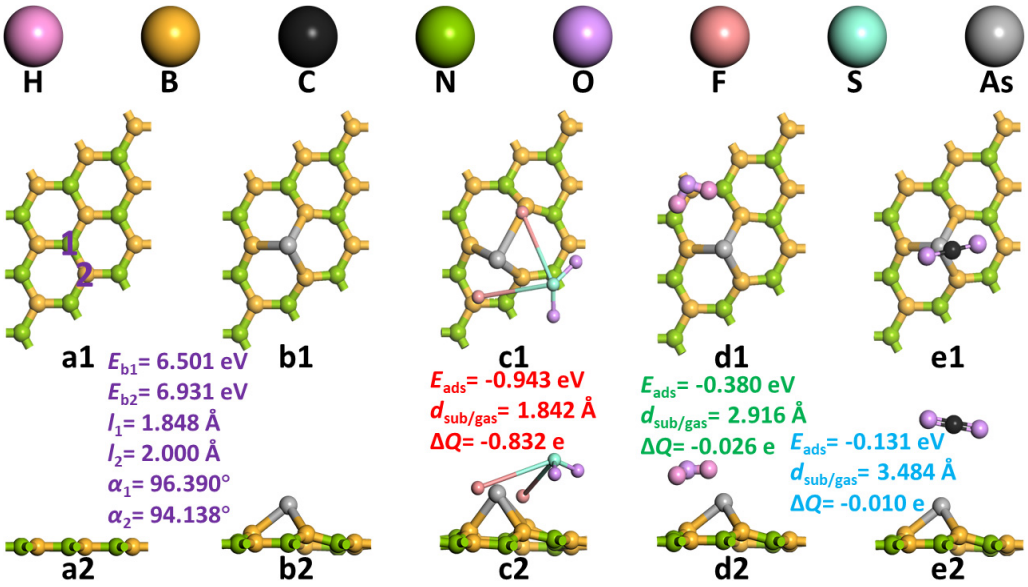

Figure 1. The geometric structures of (**a1**,**a2**) h−BN monolayer, (**b1**,**b2**) As−BN monolayer, (**c1**,**c2**) SO_2F_2 adsorption system, (**d1**,**d2**) H_2O adsorption system, (**e1**,**e2**) CO_2 adsorption system.

Three gases (SO_2F_2, H_2O, and CO_2) were close to the As-BN monolayer from different orientations and positions to obtain the optimal adsorption configuration, as shown in Figure 1(c1–e2). In order to quantify the adsorption of As-BN monolayer on various gases, the adsorption energies (E_{ads}), the nearest distance of gas molecules to the substrate ($d_{sub/gas}$), and the transfer charge (ΔQ) were calculated.

From the perspective of adsorption energy, the adsorption energy of the three adsorption systems is negative, and the adsorption effect of the As-BN monolayer on SO_2F_2 gas molecules is significantly stronger than that of the other two gas molecules. This indicates that the three adsorption reactions are exothermic and spontaneous, and the adsorption effect of the As-BN monolayer on SO_2F_2 gas molecules is particularly strong. In general, we consider that an adsorption energy of less than −0.6 eV is chemical adsorption. This means that the adsorption time and detection time of an As-BN monolayer for SO_2F_2 gas molecules will reach a good balance. The other two gases may be desorbed from the As-BN monolayer without an electrical signal display. This proves the specificity of the As-BN monolayer for SO_2F_2 adsorption. From a geometrical point of view, the As-BN monolayer adsorption of SO_2F_2 gas molecules is more obvious than the change in H_2O gas molecules and CO_2 gas molecules, as shown in Figure 1(c1–e2). Before and after adsorption, the bond lengths of SO_2F_2, H_2O, and H_2O molecules changed from 1.613 Å of S-F bond length to 3.724 Å, 0.97 Å of H-O bond length to 0.972Å, and 1.176 Å of C=O bond length to 1.175 Å, respectively. It can be found that the change of bond angle is also similar, and the geometric configuration change of the SO_2F_2 gas molecule is more obvious than that of the other two gases. At the same time, the shortest distance between SO_2F_2 gas molecules and the substrate is also smaller. This indicates that the adsorption of SO_2F_2 gas molecules on the As-BN monolayer is closer and stronger, which may lead to a more obvious electrical signal response of the As-BN monolayer. It is worth mentioning that the shortest distance between the three gas molecules and the substrate is the shortest distance between an atom of the gas molecule and an As atom. This indicates that doping an As atom to replace an N atom will significantly improve the gas-sensing adsorption capacity of the substrate. From the perspective of transfer charge, the transfer charge of the SO_2F_2 gas adsorption system is 40 and 80 times that of the other two adsorption systems. This will make the electrical signal response of the As-BN monolayer before and after the adsorption of different gases show obvious differences. Therefore, from the above point of view, compared with CO_2 gas molecules and H_2O gas molecules, the As-BN monolayer can achieve good specificity detection for SO_2F_2 gas molecules.

In order to further explore the electronic behavior of each model, we calculated their total density of states (TDOS), electron localization-focusing function (ELF), and charge difference density (CDD), as shown in Figure 2. Figure 2a describes the TDOS of the substrate before and after doping. It can be seen that the As atom doped As-BN monolayer TDOS overall moves to the lower left energy direction, but the change of the peak size is relatively small, indicating that the doped As atoms have no significant effect on the crystal structure of the substrate. Continuous TDOS means that the As-BN monolayer has good conductivity. The TDOS of the As-BN monolayer has an obvious peak at the Fermi level, indicating that the energy gap of the As-BN monolayer doped with an As atom instead of an N atom is smaller than that of the h-BN monolayer, which makes electrons more prone to transition. Therefore, the doping of As atoms is beneficial to improving the conductivity of the h-BN monolayer. At the same time, there are different degrees of hybridization and overlap in some energy levels, which shows that As atoms can form a stable doping structure with an h-BN monolayer.

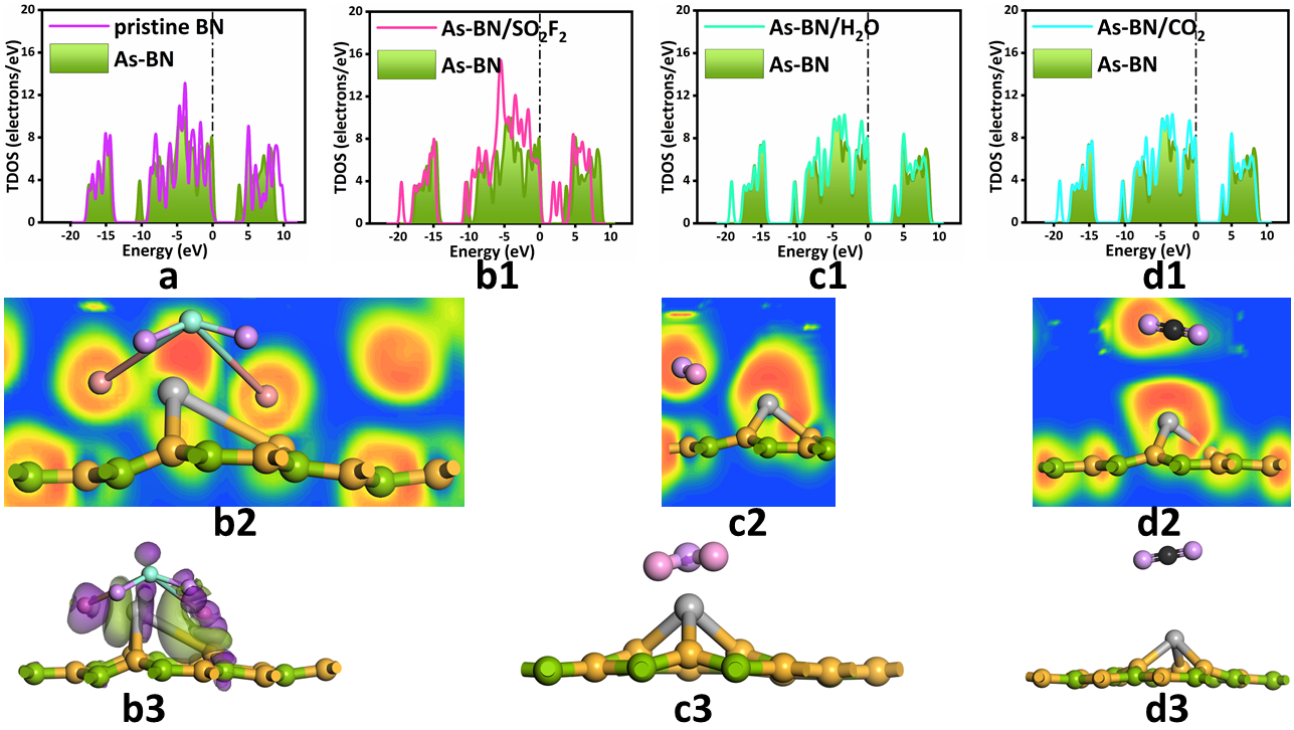

Figure 2. (**a**) The TDOS of h−BN monolayer and As−BN monolayer. The TDOS, ELF, and CDD of (**b1**–**b3**) SO_2F_2 adsorption system, (**c1**–**c3**) H_2O adsorption system, (**d1**–**d3**) CO_2 adsorption system. The Fermi level is set at zero.

Figure 2(b1,c1,d1) shows the TDOS of three gas adsorption systems. Compared with the other two adsorption systems, the change of TDOS in the SO_2F_2 gas adsorption system before and after adsorption is more obvious, as shown in Figure 2(b1). Near the Fermi level, TDOS changes significantly, which enhances the electron co-ownership movement around SO_2F_2 gas molecules and enhances the electron transition ability between the valence band and conduction band. The electrical conductivity of the system was significantly improved. At the same time, TDOS increases significantly at the far Fermi level, which may also contribute to conductivity. However, the TDOS of the other two adsorption systems did not change significantly before and after adsorption, especially near the Fermi level. This indicates that it is difficult to monitor the adsorption of H_2O or CO_2 molecules on the As-BN monolayer surface. Even if there are new peaks or some changes in TDOS far away from the Fermi level, the contribution to conductivity is negligible. This is also consistent with the small adsorption energy of these two gas molecules in the adsorption process.

The above analysis was also confirmed in the ELF and CDD of the three adsorption systems, as shown in Figure 2(b2,b3). The fusion of orange and green regions indicates that the F atom and As atom of the SO_2F_2 gas molecule have strong mutual attraction, and the electron density increases significantly, but the two are obviously not completely fused. Combined with the adsorption effect in the SO_2F_2 adsorption system previously analyzed, the adsorption between SO_2F_2 gas molecules and As-BN monolayer is more likely to be between physical adsorption and chemical adsorption. Figure 2(c2,d2) showed that the ELF of the H_2O adsorption system and CO_2 adsorption system also tend to converge, but this trend is weaker than that of the SO_2F_2 adsorption system. Therefore, combined with the previous adsorption energy, transfer charge, and geometric configuration parameters, the adsorption between the H_2O gas molecule and the CO_2 gas molecule and the As-BN monolayer were determined as physical adsorption. In the CDD of the SO_2F_2 gas adsorption system, there are dense electron concentration areas and electron dissipation areas around gas atoms and As atoms, as shown in Figure 2(b3). This indicates that the adsorption reaction of the two is accompanied by intense charge transfer. This is also very consistent with the previously calculated charge transfer (−0.832 e). At the same time, the atoms of SO_2F_2 gas molecules are more surrounded by electron concentration areas, which is also consistent with the negative charge transfer calculated previously. The SO_2F_2 gas molecule is an electron acceptor, and the As-BN monolayer is an electron donor. However, the electron-dissipation region and electron-aggregation region of the other two adsorption systems are not obvious at the same isosurface value as the SO_2F_2 adsorption system. This proves that the charge transfer between H_2O and CO_2 molecules interacting with the As-BN monolayer is very small. This is consistent with the previous calculation of charge transfer; that is, the charge transfer of the H_2O adsorption system and the CO_2 adsorption system is much smaller than that of SO_2F_2. Therefore, in the three adsorption systems, the adsorption and electronic behavior of the As-BN monolayer on SO_2F_2 gas molecules are particularly strong.

For resistive gas sensors, it is necessary to detect SO_2F_2 gas molecules when the conductivity changes properly. Band energy has a significant correlation with the conductivity of the system. When the band gap increases, the conductivity of the system decreases; when the band gap decreases, the conductivity of the system increases. The larger the band gap, the harder it is for electrons to enter the conduction band. Reflected in the macro are the current or voltage changes. It can be seen from Figure 3a,b that the band gap of the As-BN monolayer doped with As atoms decreased significantly from 4.658 eV to 3.695 eV. The decrease in the band gap means that the electron transition will be easier, and the change in the conductivity of the material may be more obvious. As shown in Figure 3b–f, after the adsorption of the SO_2F_2 gas molecules, the energy gap value of the system changes significantly and is significantly different from that of the other two adsorption systems, and the band gap energy decreases by nearly 50%. The absolute values of the band gap energy changes of the other two adsorption systems are less than 0.6%, which is very difficult in the actual detection. The specificity of the As-BN monolayer for SO_2F_2 gas molecular detection was also proved. At the same time, we consider that SF_6 is more likely to decompose into characteristic gases such as SO_2F_2 under the condition of micro-water. Therefore, the distinguishing detection of H_2O and SO_2F_2 gas molecules are particularly important in SF_6 decomposition gas detection. Therefore, the As-BN monolayer is very suitable for the detection of SF_6 decomposition gases.

In order to further explore the practical potential of the As-BN monolayer gas sensor, the sensitivity (S) and recovery time (τ) of three adsorption systems were calculated. Sensitivity is an important performance index of gas sensors, which is closely related to the change of band energy gap of the system. Recovery time is an important parameter to describe the desorption rate of the gas sensor to the target gas, which is closely related to the adsorption energy when the gas sensing material interacts with the measured gas. Figure 4a shows the recovery time of three adsorption systems. The results showed that the recovery time was from 44.7 s to 0.862 s at the temperature of 358 K to 398 K. This was

because the adsorption and desorption of the As-BN monolayer and SO_2F_2 gas were easier with the increase in temperature due to the addition of external energy. At the same time, the recovery time of the other two adsorption systems is shorter. This makes it impossible for the As-BN monolayer to effectively adsorb and respond to H_2O or CO_2 gas molecules in practical applications. This is very useful for the specific detection of SO_2F_2 gas. As shown in Figure 4b, the SO_2F_2 gas adsorption system shows high sensitivity at various temperatures. The sensitivity is 4.38×10^{14} at room temperature (298 K). At 398 K, the sensitivity of the As-BN monolayer gas sensor can also reach 9.17×10^{10}. This means that in the early stage of PD, the As-BN monolayer gas sensor can detect SO_2F_2 gas in time, which provides the possibility for early warning. In conclusion, the As-BN monolayer has great potential for the detection of SF_6 decomposition gases.

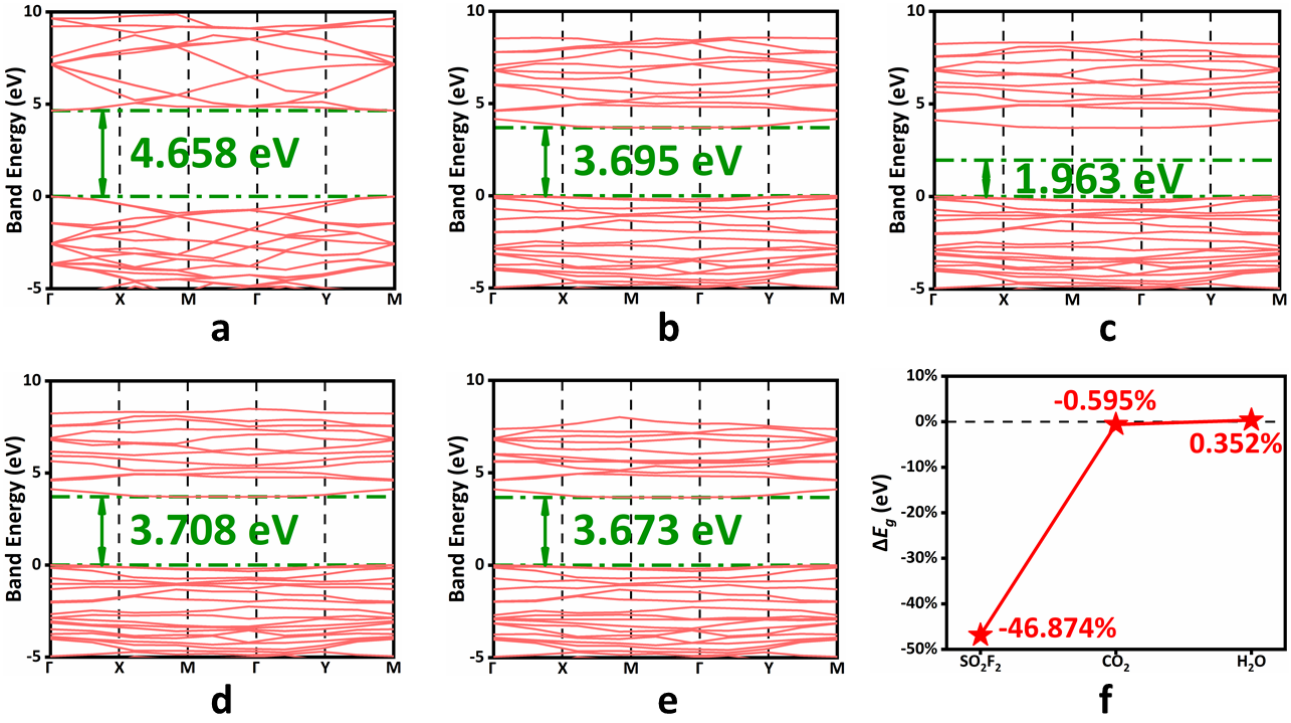

Figure 3. The band energy of (**a**) h−BN monolayer, (**b**) As−BN monolayer, (**c**) SO_2F_2 adsorption system, (**d**) H_2O adsorption system, (**e**) CO_2 adsorption system. (**f**) The ΔE_g of three adsorption systems.

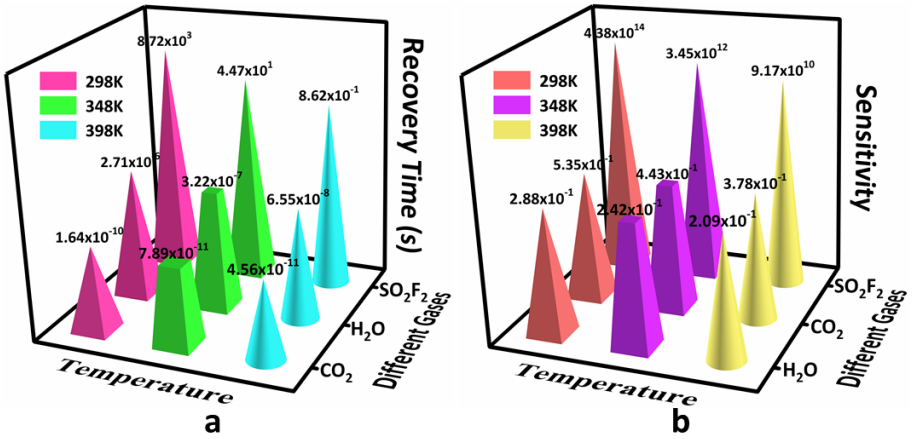

Figure 4. The (**a**) recovery time and (**b**) sensitivity of three adsorption systems.

4. Conclusions

In this study, the h-BN monolayer, As-BN monolayer, and three gas molecular models (SO_2F_2, H_2O, and CO_2) were established, and the optimal adsorption structures of the three gases were obtained through calculation and analysis. On this basis, by calculating the adsorption energy, geometric structure parameters, transfer charge, adsorption energy, TDOS, ELF, CDD, band structure, recovery time, and sensitivity of each system, the possibility of an As-BN monolayer as a sensitive layer to detect the important characteristic gas SO_2F_2 in SF_6 decomposition gases was analyzed. The calculation results show that in the three adsorption systems, the parameters of the SO_2F_2 adsorption system are more appropriate and significantly different from those of the other two adsorption systems, which ensures the specificity of the As-BN monolayer for the detection of SO_2F_2 gas molecules. At the same time, at multiple temperatures. The detection of SO_2F_2 gas molecules by the As-BN monolayer can ensure high sensitivity and short recovery time. Therefore, this study not only provides a theoretical basis for the preparation of As-BN monolayer gas sensors for SF_6 decomposition gas monitoring but also provides a convenient way for the development of other sensors.

Author Contributions: Conceptualization, L.-Y.G.; software, Z.H.; validation, L.-Y.G.; writing—original draft preparation, Y.L.; writing—review and editing, Y.T.; supervision, S.-Y.X.; funding acquisition, Y.T. All authors have read and agreed to the published version of the manuscript.

Funding: This research was funded by the National Key Research and Development Program 2018YFB2100100.

Institutional Review Board Statement: Not applicable.

Informed Consent Statement: Not applicable.

Data Availability Statement: Not applicable.

Conflicts of Interest: The authors declare no conflict of interest.

References

1. Purnomoadi, A.; Mor, A.R.; Smit, J. Spacer flashover in Gas Insulated Switchgear (GIS) with humid SF_6 under different electrical stresses. *Int. J. Electr. Power Energy Syst.* **2020**, *116*, 105559. [CrossRef]
2. Xing, Y.; Liu, L.; Xu, Y.; Yang, Y.; Li, C. Defects and failure types of solid insulation in gas insulated switchgear: In situ study and case analysis. *High Volt* **2021**, *7*, 158–164. [CrossRef]
3. Khan, Q.; Refaat, S.S.; Abu-Rub, H.; Toliyat, H.A. Partial discharge detection and diagnosis in gas insulated switchgear: State of the art. *IEEE Electr. Insul. Mag.* **2019**, *35*, 16–33. [CrossRef]
4. Li, X.; Liu, W.; Xu, Y.; Ding, D. Partial Discharge and Movement Characteristics of Micron-sized Metal Particles on Insulator Surface in Gas-Insulated Switchgear with Long-time AC Stress. *IEEE Trans. Dielectr. Electr. Insul.* **2021**, *28*, 2152–2160. [CrossRef]
5. Zhou, H.Y.; Ma, G.M.; Wang, Y.; Qin, W.Q.; Jiang, J.; Yan, C.; Li, C.R. Optical sensing in condition monitoring of gas insulated apparatus: A review. *High Volt.* **2019**, *4*, 259–270. [CrossRef]
6. Wu, S.; Zeng, F.; Tang, J.; Yao, Q.; Miao, Y. Triangle fault diagnosis method for SF_6 gas-insulated equipment. *IEEE Trans. Power Deliv.* **2019**, *34*, 1470–1477. [CrossRef]
7. Pang, X.; Wu, H.; Pan, J.; Qi, Y.; Li, X.; Zhang, J.; Xie, Q. Analysis of Correlation between Internal discharge in GIS and SF_6 Decomposition Products. In Proceedings of the 2018 IEEE International Conference on High Voltage Engineering and Application (ICHVE), Athens, Greece, 10–13 September 2018; pp. 1–4.
8. Zeng, F.; Tang, J.; Zhang, X.; Zhou, S.; Pan, C.; Sánchez, R. Typical internal defects of gas-insulated switchgear and partial discharge characteristics. In *Simulation and Modelling of Electrical Insulation Weaknesses in Electrical Equipment*; InTech: Rijeka, Croatia, 2018; p. 103.
9. Miao, Y.; Li, C.; Yao, Q.; Hou, Y.; Zeng, F. Study on Influencing Factors of SF_6 Decomposition Products Detection Results. In Proceedings of the 2020 IEEE International Conference on High Voltage Engineering and Application (ICHVE), Beijing, China, 6–10 September 2020; pp. 1–4.
10. Hao, Y.; Jin, S.; Li, X.; Tian, H.; Liu, Z.; Liu, P.; Peng, Z. Study on Gas-tightness detection analysis and leak test of UHV AC GIL. In Proceedings of the 16th IET International Conference on AC and DC Power Transmission (ACDC 2020), Online, 2–3 July 2020; pp. 2155–2159.
11. Wang, J.; Yang, G.; Xue, J.; Lei, J.; Cai, Q.; Chen, D.; Lu, H.; Zhang, R.; Zheng, Y. High sensitivity and selectivity of AsP sensor in detecting SF_6 decomposition gases. *Sci. Rep.* **2018**, *8*, 12011.

12. Wang, H.; Yang, J.; Li, F.; Liu, W.; Liang, H. Feature Fingerprint Extraction and Abnormity Diagnosis Method of the Vibration on the GIS. In Proceedings of the 2020 IEEE International Conference on High Voltage Engineering and Application (ICHVE), Beijing, China, 6–10 September 2020; pp. 1–4.
13. Cho, I.; Sim, Y.C.; Cho, M.; Cho, Y.-H.; Park, I. Monolithic micro light-emitting diode/metal oxide nanowire gas sensor with microwatt-level power consumption. *ACS Sens.* **2020**, *5*, 563–570. [CrossRef]
14. Yan, W.; Liu, Y.; Shao, G.; Zhu, K.; Cui, S.; Wang, W.; Shen, X. Chemical surface adsorption and trace detection of alcohol gas in graphene oxide-based acid-etched SnO_2 aerogels. *ACS Appl. Mater. Interfaces* **2021**, *13*, 20467–20478. [CrossRef]
15. Mondal, B.; Gogoi, P.K. Nanoscale Heterostructured Materials Based on Metal Oxides for a Chemiresistive Gas Sensor. *ACS Appl. Electron. Mater.* **2022**, *4*, 59–86. [CrossRef]
16. Choi, J.H.; Lee, J.; Byeon, M.; Hong, T.E.; Park, H.; Lee, C.Y. Graphene-based gas sensors with high sensitivity and minimal sensor-to-sensor variation. *ACS Appl. Nano Mater.* **2020**, *3*, 2257–2265. [CrossRef]
17. Li, X.; Scully, R.A.; Shayan, K.; Luo, Y.; Strauf, S. Near-unity light collection efficiency from quantum emitters in boron nitride by coupling to metallo-dielectric antennas. *ACS Nano* **2019**, *13*, 6992–6997. [CrossRef] [PubMed]
18. Li, L.; Wei, C.; Song, H.; Yang, Y.; Xue, Y.; Deng, D.; Lv, Y. Cataluminescence coupled with photoassisted technology: A highly efficient metal-free gas sensor for carbon monoxide. *Anal. Chem.* **2019**, *91*, 13158–13164. [CrossRef] [PubMed]
19. Zhang, T.; Pan, W.; Zhang, Z.; Qi, N.; Chen, Z. Theoretical Study of Small Molecules Adsorption on Pristine and Transition Metal Doped GeSe Monolayer for Gas Sensing Application. *Langmuir* **2022**, *38*, 1287–1295. [CrossRef]
20. Modi, G.; Stach, E.A.; Agarwal, R. Low-Power Switching through Disorder and Carrier Localization in Bismuth-Doped Germanium Telluride Phase Change Memory Nanowires. *ACS Nano* **2020**, *14*, 2162–2171. [CrossRef]
21. Guo, L.-Y.; Xia, S.-Y.; Sun, H.; Li, C.-H.; Long, Y.; Zhu, C.; Gui, Y.; Huang, Z.; Li, J. A DFT Study of the Ag-Doped h-BN Monolayer for Harmful Gases (NO_2, SO_2F_2, and NO). *Surf. Interfaces* **2022**, 102113. [CrossRef]
22. Agrawal, A.V.; Kumar, N.; Kumar, M. Strategy and future prospects to develop room-temperature-recoverable NO_2 gas sensor based on two-dimensional molybdenum disulfide. *Nano-Micro Lett.* **2021**, *13*, 38. [CrossRef]
23. Roondhe, B.; Dabhi, S.D.; Jha, P.K. Sensing properties of pristine boron nitride nanostructures towards alkaloids: A first principles dispersion corrected study. *Appl. Surf. Sci.* **2018**, *441*, 588–598. [CrossRef]
24. Guo, L.-Y.; Xia, S.-Y.; Tan, Y.; Huang, Z. Zr-Doped h-BN Monolayer: A High-Sensitivity Atmospheric Pollutant-Monitoring Sensor. *Sensors* **2022**, *22*, 4103. [CrossRef]
25. Alzate-Carvajal, N.; Luican-Mayer, A. Functionalized graphene surfaces for selective gas sensing. *ACS Omega* **2020**, *5*, 21320–21329. [CrossRef]
26. Xia, S.-Y.; Tao, L.-Q.; Jiang, T.; Sun, H.; Li, J. Rh-doped h-BN monolayer as a high sensitivity SF_6 decomposed gases sensor: A DFT study. *Appl. Surf. Sci.* **2021**, *536*, 147965. [CrossRef]
27. Sharma, B.; Sharma, A.; Myung, J.-H. Selective ppb-level NO_2 gas sensor based on SnO_2-boron nitride nanotubes. *Sens. Actuator B Chem.* **2021**, *331*, 129464. [CrossRef]
28. Guo, L.-Y.; Liang, S.; Yang, Z.; Jin, L.; Tan, Y.; Huang, Z. Gas-Sensing Properties of Dissolved Gases in Insulating Material Adsorbed on SnO_2-GeSe Monolayer. *Chemosensors* **2022**, *10*, 212. [CrossRef]
29. Schleicher, M.; Fyta, M. Lateral MoS_2 heterostructure for sensing small gas molecules. *ACS Appl. Electron. Mater.* **2019**, *2*, 74–83. [CrossRef]
30. Jia, Z.; Gao, Z.; Feng, A.; Zhang, Y.; Zhang, C.; Nie, G.; Wang, K.; Wu, G. Laminated microwave absorbers of A-site cation deficiency perovskite $La_{0.8}FeO_3$ doped at hybrid RGO carbon. *Compos. Part B-Eng.* **2019**, *176*, 107246. [CrossRef]
31. Chen, W.Y.; Yen, C.-C.; Xue, S.; Wang, H.; Stanciu, L.A. Surface functionalization of layered molybdenum disulfide for the selective detection of volatile organic compounds at room temperature. *ACS Appl. Mater. Interfaces* **2019**, *11*, 34135–34143. [CrossRef]
32. Wang, G.; Yu, J.; Zheng, K.; Huang, Y.; Li, X.; Chen, X.; Tao, L.-Q. A monolayer composite of h-BN doped by a nano graphene domain: As sensitive material for SO_2 gas detection. *IEEE Electron Device Lett.* **2020**, *41*, 1404–1407. [CrossRef]
33. Peng, Z.; Tao, L.-Q.; Wang, G.; Zhang, F.; Sun, H.; Zhu, C.; Zou, S.; Yu, J.; Chen, X. The promotion of sulfuric vacancy in two-dimensional molybdenum disulfide on the sensing performance of SF6 decomposition components. *Appl. Surf. Sci.* **2022**, *571*, 151377. [CrossRef]
34. Liu, Y.; Gui, Y.; Xu, L.; Chen, X. Adsorption property of Co, Rh, and Pd-embedded g-C_3N_4 monolayer to SO_2F_2 gas. *J. Mater. Res. Technol.-JMRT* **2021**, *15*, 4790–4799. [CrossRef]
35. Zhang, D.; Wu, J.; Li, P.; Cao, Y. Room-temperature SO_2 gas-sensing properties based on a metal-doped MoS nanoflower: An experimental and density functional theory investigation. *J. Mater. Chem. A* **2017**, *5*, 20666–20677. [CrossRef]
36. Zhang, D.; Li, Q.; Li, P.; Pang, M.; Luo, Y. Fabrication of Pd-decorated $MoSe_2$ nanoflowers and density functional theory simulation toward ammonia sensing. *IEEE Electron Device Lett.* **2019**, *40*, 616–619. [CrossRef]